Research Journal of Applied Sciences, Engineering and Technology 6(21): 3964-3973, 2013
DOI:10.19026/rjaset.6.3497
ISSN: 2040-7459; e-ISSN: 2040-7467

Submitted: January 24, 2013 Accepted: March 07, 2013 Published: November 20, 2013

Research Article

Structure Construction and Position Signals Analysis of the Single-Axis Piezoelectric Actuated Stage by using a novel Piezoelectric Actuator

Shann-Chyi Mou
Department of Mechanical Engineering, Chien Hsin University of Science and Technology, Zhongli 32097, Taiwan, R.O.C

Abstract: In this study, a novel piezoelectric actuator structure -4-9-9-14 piezoelectric actuator is constructed and it is made of piezoelectric buzzer to drive a piezoelectric actuated stage. The 4-9-9-14 piezoelectric actuator offers a better balanced capability of forward rotation and reverse rotation than the conventional edge-driving piezoelectric actuator. According to the rotational speed experiment, the CW/CCW ratio of the 4-9-9-14 piezoelectric actuator is probably 1: 0.8. The movement of the piezoelectric actuated stage is read and analyzed by means of data acquisition card and LabVIEW software operating in conjunction with a linear encoder. In a natural environment, plenty of noise interferes with linear encoder signals and results in erroneous addition performed by a counter. Therefore, the LabVIEW program set forth the means of filtering and the method for retrieving a correct position signal. The piezoelectric actuated stage by using 4-9-9-14 piezoelectric actuator can be expanded and applied easily to a longer distance moved stage.

Keywords: Buzzer, data acquisition, LabVIEW, linear encoder, piezoelectric actuated stage, piezoelectric actuator

INTRODUCTION

Due to technological advancements, a wide variety of motors are in use in different fields. Motors nowadays are no longer restricted to those driven by an electromagnetic force, as an unorthodox type of motors, namely piezoelectric ultrasonic motors (or known as piezoelectric motors for short), has emerged thanks to the rapid development of material technology in recent years. A linear mechanical mechanism used to perform linear translation mostly by a conventional rotary motor that operates in conjunction with ball screws. However, ball screws are flawed with backlash and thus are not effective in enhancing positioning precision and speed. By contrast, piezoelectric motors have advantages over conventional rotary motors. For example, piezoelectric motors feature a larger holding torque and less instability (i.e., the driven mechanism keeps moving under inertia) than conventional rotary motors. Due to its aforesaid advantages, a piezoelectric motor is capable of precise positioning. Other advantages of piezoelectric motors include: insusceptibility to an electromagnetic field, high-precision positioning, low noise (because their deceleration mechanism can work without any gear), compactness, low weight and large torque (Mou and Ouyang, 2004). In recent years, a piezoelectric motor poses a new choice of actuators in terms of precise stage positioning. In engineering-related application, stage movement precision technology has a trend toward sophistication, miniaturization, high precision and high stability and has a strict requirement for precision and stability of a driving device in particular. Hence, piezoelectric motors still have much room for development when functioning as actuators for driving stages.

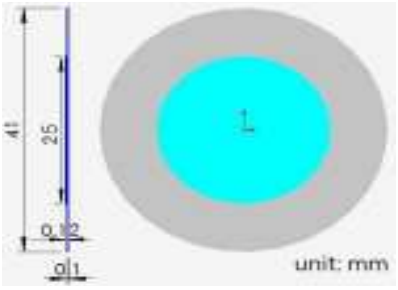

Fig. 1: The dimensions diagram of piezoelectric buzzer

PIEZOELECTRIC ACTUATORS

The piezoelectric actuator described in this study is a thinned piezoelectric actuator designed in an unorthodox way and made from a commercially-available inexpensive piezoelectric buzzer (OBO-TE41208-21) (Mou, 2012, 2013). The piezoelectric buzzer consists of a piezoelectric ceramic membrane and a thin metal plate which are glued together by silver paste as shown in Fig. 1 (Sung and Mou, 2008). Parameters of the piezoelectric buzzer are shown in Table 1 (OBO, 2013). The piezoelectric buzzer is

Table 1: The parameters table of piezoelectric buzzer

Piezoelectric buzzer parameter	Parameter value
Metallic back plate diameter	41.00 mm
Piezoelectric ceramic diameter	25.00 mm
Metallic back plate thickness	0.10 mm
Total thickness	0.22 mm
Resonance frequency	0.8±0.3 kHz
Resonance impedance	2000 Ω (max)
Capacitance value	77,000±30% pF
Metallic back panel material	nickel (Ni) alloy

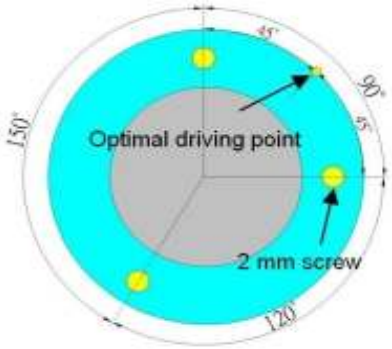

Fig. 2: The structure diagram of the 3-4-5 piezoelectric actuator

intrinsically characterized in that its radial-direction displacement vibration amplitude variation is larger than its longitudinal-direction (or axial-direction) displacement vibration amplitude variation; hence, if the piezoelectric buzzer is designed to be a mechanism for driving a rotor by radial-direction displacement vibration amplitude variation, its various characteristics will be improved (Juang and Hardtke, 2001). Therefore, our research team develops an edge-driving piezoelectric actuator (Wen *et al*., 2003; Yen *et al*., 2003) and its stator structure is shown in Fig. 2.

In the stator structure of the edge-driving piezoelectric actuator shown in Fig. 2, three round holes of a diameter of 2 mm each are cut out of a metallic (nickel alloy) back-panel of the piezoelectric buzzer, arranged in their respective orientations of 90°, 120°, 150° and locked with screws, respectively, so that the piezoelectric buzzer appears in the form of an angularly unbalanced (or asymmetric) 90°-120°-150° structure (also known as 3-4-5 structure for short). The actuation principle of the edge-driving piezoelectric actuator depends on the aforesaid asymmetric 3-4-5 structure and involves converting compulsorily a voltage signal sent to between a piezoelectric ceramic material and the metallic back-panel into a deformation wave motion comprising a mixture of a standing wave (displacement extension produced axially) and a traveling wave (displacement extension produced radially); hence, the edge-driving piezoelectric actuator can be regarded as a hybrid type piezoelectric actuator. As shown in Fig. 3(a) (Hsu and Mou, 2006), ANSYS simulation reveals: radial and rotational distortion vectors of leftward (counterclockwise) motion occurs at a peripheral position in the 90° sector, indicating that

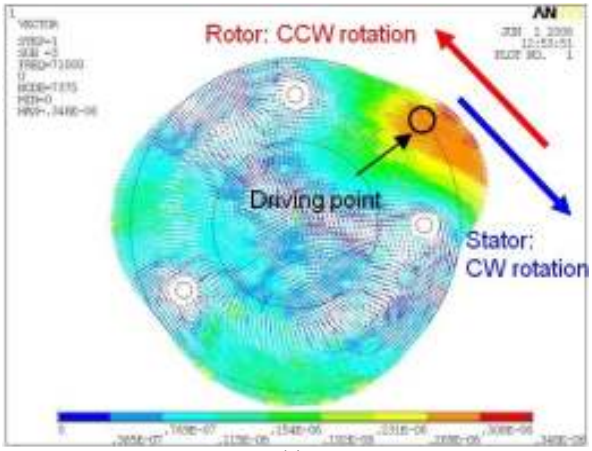

(a)

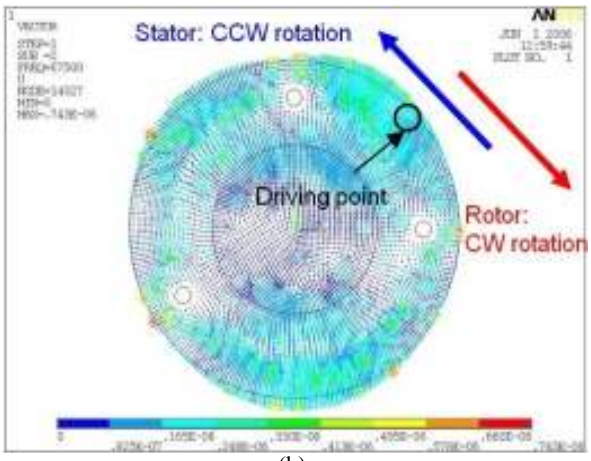

(b)

Fig. 3: The ANSYS dynamic simulation diagrams of counter of the 3-4-5 piezoelectric actuator; (a) counter clockwise rotation, (b) clockwise rotation

they are capable of driving the rotor to rotate clockwise; no peripheral position in the 120° and 150° sectors is suitable for serving as a driving point of the actuator, because the distortion vectors are attributed to a scattering motion that occurs in the directions of screws located on its two sides. The result shown in Fig. 3(b) is consistent with Fig. 3(a) except that the distortion vectors at a peripheral position in the 90° sector are rightward (clockwise), thereby indicating that they are capable of driving the rotor to rotate counterclockwise. Switching the edge-driving piezoelectric actuator between forward rotation and reverse rotation is achieved by alteration of two driving frequencies rather than conventional alteration of a phase difference from a dual-phase driving power source; hence, determination of the forward and reverse rotation driving frequencies of the actuator is of vital importance.

Unlike a conventional piezoelectric actuator, the edge-driving piezoelectric actuator does not have any alternately polarized electrodes; hence, the forward rotation and reverse rotation of the actuator take place

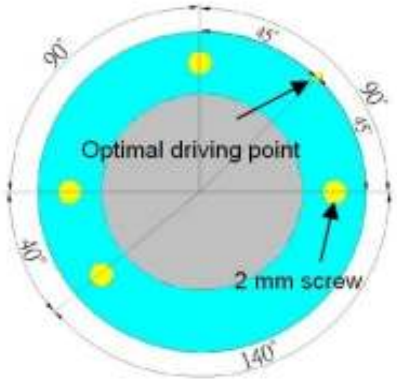

Fig. 4: The structure diagram of the 4-9-9-14 piezoelectric actuator

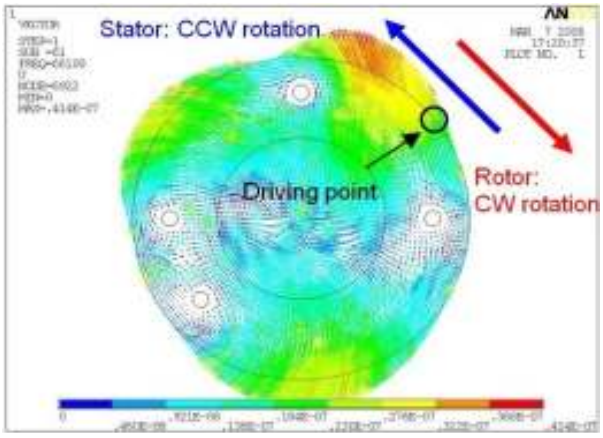

(a)

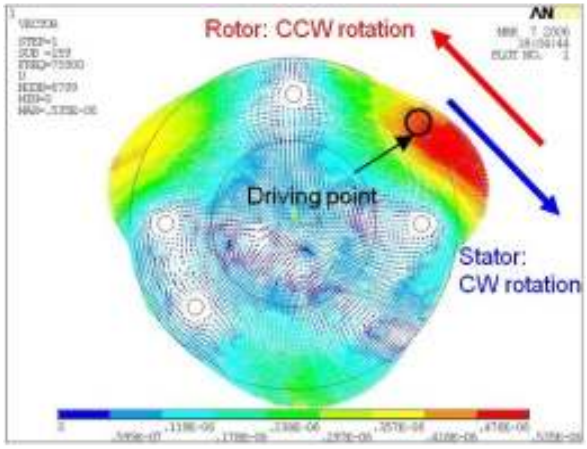

(b)

Fig. 5: The ANSYS dynamic simulation diagrams of counter of the 4-9-914 piezoelectric actuator: (a) clockwise rotation; (b) counterclockwise rotation

by means of two different driving frequencies (with one being a true resonance frequency of the system and the other being the second-best driving frequency) instead of a phase change (with one phase expressed *in-sint* and the other phase *in-cost*, or with one phase expressed *in-sint* and the other phase in cost) of a dual-phase input power source (with one phase expressed *in-sint* and the other phase *in-cost*) (Sashida and Kenjo, 1993; Ueha *et al*., 1993). However, the two different driving frequencies differ from each other in terms of the efficiency of actuation of forward rotation and reverse rotation (strong driving torque and quick rotation in one direction, but weak driving torque and notably slow rotation in the other direction). To overcome the aforesaid drawback, we modifies the prototype by balancing the forward rotation and reverse rotation of the piezoelectric actuator, which is achieved by changing its fixation point location and thus putting four fixation posts on four radii that separate a 40° sector, a 90° sector, a 90° sector and a 140° sector, respectively, as shown in Fig. 4. Therefore, the modified piezoelectric actuator is known as a 4-9-9-14 piezoelectric actuator and distortion vectors of its forward rotation and reverse rotation are depicted in Fig. 5(a, b) (Mou, 2011). The aforesaid modification equalizes the actuation of forward rotation and reverse rotation. The experiment proves that the aforesaid design reduces the difference in actuation between forward rotation and reverse rotation greatly (Jheng and Mou, 2008).

ROTATIONAL SPEED MEASURED STAGE

In this section we will carry out the rotational speed measurements so that we could observe the performances of the 3-4-5 and 4-9-9-14 piezoelectric actuators. There are three main part of the rotational speed measured stage which is used to measure the actuator capability, include the actuator (stator mechanism), the preload propelled mechanism and the rotor.

The design of actuator is fixed locking up on the stage base. As shown in Fig. 6(a), the middle part is an adjustable angle (θ) and radius (r) of the actuator holder. In the preload propelled mechanism part, the micrometer is used to push the rotor and provide the appropriate preload to make a little contact between actuator and rotor. The holder of the micrometer and the fixed micrometer are shown in Fig. 6(b). In addition, rotor and the actuator are depended on friction to drive; it causes abrasion because of long time operating and the gap is generated. That's the reason that we design the preload propelled mechanism to give an impetus to the rotor by micrometer through the fixed actuator (stator mechanism). Whenever the abrasion is oversized which means the gaps of actuator and rotor are non-contact that would influence the actuator of the capability of promoting the rotor.

Then the contact with rotor and the actuator would be returned to a better condition through the preload propelled mechanism. In the rotor part, as shown in

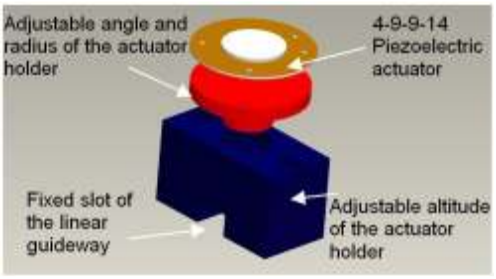

(a)

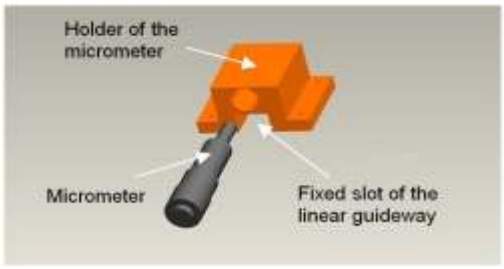

(b)

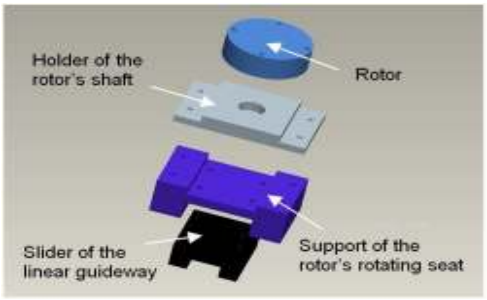

(c)

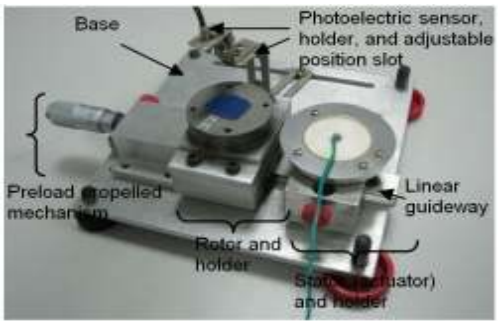

(d)

Fig. 6: (a) The sketch map of the actuator stator's fixed structure, (b) the sketch map of the preload propelled mechanism, (c) the sketch map of the rotor, (d) the stereogram of a rotational speed measured stage of rotational speed measured stage is shown in Fig. 6(d).

Fig. 6(c) from the top to the bottom are the rotor, holder of the rotor's shaft, support of the rotor's and slider of the linear guide way. The slider of the linear guide way

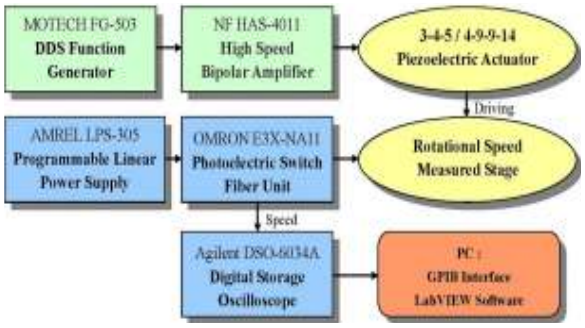

(a)

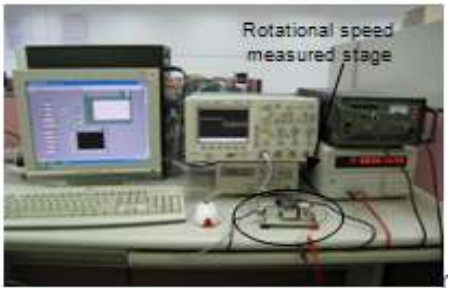

(b)

Fig. 7: (a) The sketch map of a rotational speed measured system, (b) the stereogram of a rotational speed measured system

is locked up on the support of the rotor's rotating seat so that the slider would be moved straightly and the rotor would not be deviated as it is moved. The rotational speed measured stage is made of aluminum for easy processing. Due to the actuator is very thin, the interface surface of rotor and actuator would be cut a channel easily, thus the actuator would fall into the channel and increase friction drag but decrease capability of actuator so that the result of rotational speed measurement would be getting worse. Consequently, we do the anodizing treatment on the rotor surface to increase its hardness. The stereogram of rotational speed measured stage is shown in Fig. 6(d).

SYSTEM STRUCTURE

The process of experiment structure is shown in Fig. 7(a). The rotational speed measured system is an open-loop system. User control the driving frequency, voltage amplitude and waveform of actuating signal from function generator, enlarging 10 times with power amplifier, driving actuator to rotate rotor, measuring the rotational speed with photoelectric switch (sensor) and sending back to the PC by GPIB (general purpose interface bus) interface of the oscilloscope to obtain the correct rotational speed data. The stereogram of experiment structure of the rotational speed measured system is shown in Fig. 7(b).

Table 2: The relation between driving voltage with rotational speed of 3-4-5 piezoelectric actuator during the no-load condition

Rotor Direction (CW/CCW)	Driving Frequency (kHz)	Driving Voltage (V_{p-p})	Rotational Speed (rpm)
CW/CCW	72.3/86.0	20	355/ 23
CW/CCW	72.3/86.0	30	534/ 34
CW/CCW	72.3/86.0	40	679/ 50

Table 3:`The relation between driving voltage with rotational speed of 4-9-9-14 piezoelectric actuator during the no-load condition

Rotor Direction (CW/CCW)	Driving Frequency (kHz)	Driving Voltage (V_{p-p})	Rotational Speed (rpm)
CW/CCW	68.3/73.3	20	217/280
CW/CCW	68.3/73.3	30	279/334
CW/CCW	68.3/73.3	40	338/400

Table 4: The relation between driving voltage with rotational speed of 4-9-9-14 piezoelectric actuator during the 50 g load condition

Rotor Direction (CW/CCW)	Driving Frequency (kHz)	Driving Voltage (V_{p-p})	Rotational Speed (rpm)
CW/CCW	68.3/73.3	20	213/275
CW/CCW	68.3/73.3	30	276/329
CW/CCW	68.3/73.3	40	327/393

Table 5: The relation between driving voltage with rotational speed of 4-9-9-14 piezoelectric actuator during the 100 g load condition

Rotor direction (CW/CCW)	Driving frequency (kHz)	Driving voltage (V_{p-p})	Rotational speed (rpm)
CW/CCW	68.3/73.3	20	203/245
CW/CCW	68.3/73.3	30	250/304
CW/CCW	68.3/73.3	40	313/385

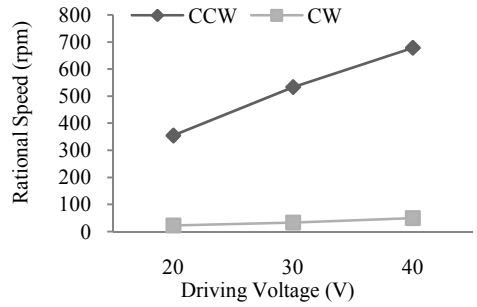

(a)

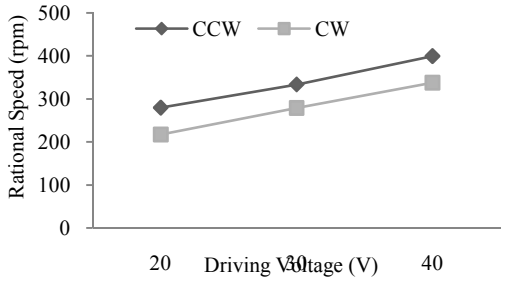

(b)

Fig. 8: The relations between driving voltage with rotational speed: (a) 3-4-5 piezoelectric actuator; (b) 4-9-9-14 piezoelectric actuator

Rotational speed measurement: We do the no-load rotational speed measurement on 3-4-5 piezoelectric actuator and change its voltage amplitude 20 V_{p-p}, 30 V_{p-p}, 40 $V_{p-p.}$ The operating frequency in 72.3 kHz is clockwise and 86 kHz is counterclockwise.

Table 6: The relation between driving voltage with rotational speed of 4-9-9-14 piezoelectric actuator during the 200 g load condition

Rotor direction (CW/CCW)	Driving frequency (kHz)	Driving voltage (V_{p-p})	Rotational speed (rpm)
CW/CCW	68.3/73.3	20	153/220
CW/CCW	68.3/73.3	30	219/280
CW/CCW	68.3/73.3	40	290/367

Table 7: The ratio statistics of clockwise and counterclockwise for 4-9-9-14 piezoelectric actuator

	Driving voltage (V_{p-p})		
Load (g)	20	30	40
0	0.775	0.835	0.845
50	0.775	0.839	0.832
100	0.829	0.822	0.813
200	0.695	0.782	0.790

Table 8: The component specifications of the piezoelectric actuated stage

Component	Material	Dimensions (mm)
4-9-9-14 Piezoelectric actuator	Piezoelectric buzzer	Φ41×0.22
Base	Stainless steel	360×196×13
Load-carrying stage	Stainless steel	220×91×6
Wear-resistant side of the load-carrying stage	Heat treating stainless steel	220×31×6
Linear encoder		36×14.8×13.5

The measurement data of 3-4-5 piezoelectric actuator in the no-load rotational speed is shown in Table 2. On the other hand, we also do the rotational speed measurement on 4-9-9-14 piezoelectric actuator inputting the voltage amplitude 20 V_{p-p}, 30 V_{p-p}, 40 $V_{p-p.}$ The relation between driving voltage with rotational speed of 4-9-9-14 piezoelectric actuator during the no-load condition is shown in Table 3. The relation between voltage with rotational speed of 4-9-9-14 piezoelectric actuator during the 50 g, 100 g and 200 g load condition are shown in Table 4, 5 and 6.

According to the data of Table 2 and 3, it could be made into Fig. 8 (a, b). Comparing with these two figures could be found out that the clockwise and counterclockwise rotation capability of the 4-9-9-14 piezoelectric actuator is comparatively identical.

Therefore in the next experiment, the 4-9-9-14 piezoelectric actuator would be used as a driving device of the system. As we can see from Table 3 to 6, when the load of 4-9-9-14 piezoelectric actuator is heavier, its rotational speed would be slower. After integrating the ratio of clockwise and counterclockwise rotation from Table 3 to 6, we could get Table 7. As we can see, when the 4-9-9-14 piezoelectric actuator is in the same load, the voltage would be larger and the ratio of clockwise and counterclockwise rotation would be closed to 1. It represents that when the voltage is larger, the rotation of clockwise and counterclockwise would be closer.

PIEZOELECTRIC ACTUATED STAGE

In preceding description, we used the rotational speed measured stage in order to measure the characteristics of actuator. In the next chapter we will introduce the piezoelectric actuated stage to be designed for positioning application. As shown in

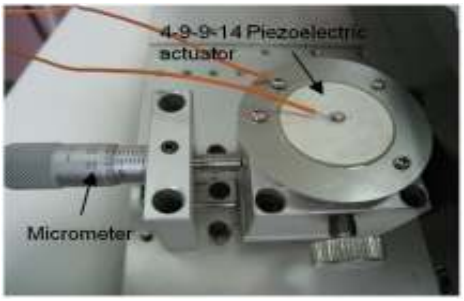

(a)

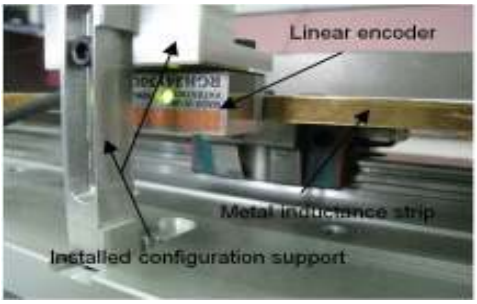

(b)

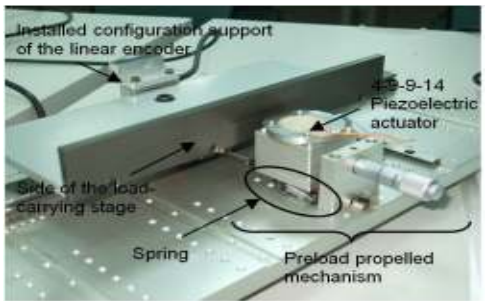

(c)

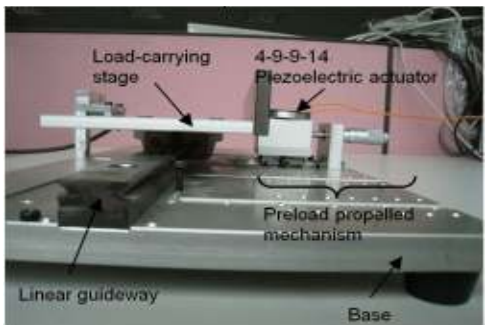

(d)

Fig. 9: (a) The stereogram of the preload propelled mechanism; (b) the installed configuration support and metal inductance strip of the linear encoder; (c) the sketch map of the piezoelectric actuated stage; (d) the side view of the piezoelectric actuated stage

Table 8, the base, the linear guideway, the linear encoder, the 4-9-9-14 piezoelectric actuator and the load-carrying stage are included in the piezoelectric actuated stage (Wen and Yen, 2007).

Except considering mechanical error, we need to understand the transmission component. The linear guideway we used in this design are mainly made of the slider, rolling bodies (balls or rollers) and guideway three parts of the composition. Its length is 360 mm and its action principle is to install the slider in the guideway to make slider do high-precision linear motion along the guideway easily by a stable movement of a ball which is between the slider and the guideway. Moreover, the characteristics include:

- **High positioning accuracy:** The friction way between the slider and the guideway is rolling friction, so the friction coefficient is very low (only 1/50 for sliding guideway). Besides, due to the difference of dynamic friction coefficient and static friction coefficient is very close, the invalidated motion would not be happened while the slider is moving and its accuracy will be up to μm level
- **High maintain accuracy:** It could be maintained the accuracy for a long time because of the very little rolling friction to the linear guideway
- **To execute high rotational speed motion by the low driving force:** The slider is moved by only using smaller actuated force because of the very little rolling friction to the linear guideway. Furthermore it's also used for high-speed motion because the heat which is generated by rolling friction is less
- **To withstand the load of each direction at the same time:** The special structure design of the linear guideway can withstand the strength for all directions

The preload propelled mechanism of the stage includes a micrometer and an actuator which are shown in Fig. 9(a). The micrometer is mainly to move actuator (stator mechanism) to the stage so that the actuator could contact slightly with the side of load-carrying stage. As a result, in an abrasion condition, recovering the contact slightly with actuator and load- carrying stage through using the micrometer could also reduce the actuator capability declining which was caused by abrasion. We designed a linear guide way setting support on the piezoelectric actuated stage because we need to do the position measurement by linear guide way which is shown in Fig. 9(b). As shown in Fig. 9(b), you can see the edge of the load-carrying stage which is stick on the metal inductance strip so that the moving condition could be inducted correctly by linear encoder. The stereogram of piezoelectric actuated stage, which was produced, assembled and completed the stage by manufacturers, is shown in Fig. 9(c). The side view of piezoelectric actuated stage is shown in Fig. 9(d). After finishing stage test, the load-carrying stage would slant a little bit when the stage is moved to both terminals by

Fig. 10: There is an askew condition between the load-carrying stage and 4-9-9-14 piezoelectric actuator

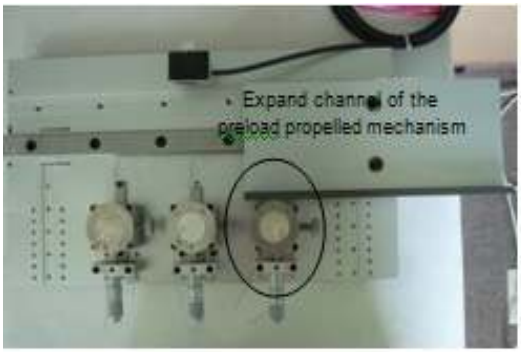

Fig. 11: The stereogram of a long distance piezoelectric actuated stage

piezoelectric actuator which is shown in Fig. 10. However, this is a problem we didn't considerate in the beginning when we designed the stage.

The 4-9-9-14 piezoelectric actuator should be changed when the abrasion which is generated by actuator is too serious. Thus we set a spring under the preload propelled mechanism which is shown in Fig. 9(c). Furthermore the stator mechanism would be removed automatically from the load-carrying stage so that it would easy to exchange the piezoelectric actuator when the micrometer is receded. In the stage designing, we have planned five expand channels of the preload propelled mechanism device in total. As shown in Fig. 11, it is the stereogram for using three preload propelled mechanisms. Consequently, the load-carrying stage can be moved longer distance by using the more preload propelled mechanisms.

POSITION SIGNALS ANALYSIS

In the stage positioning control, position sensor is a very important part, the control of convergence results would be influenced directly by the accuracy of the position signal. Therefore we must have some certain requirements and considerations on choosing the position sensor. During our experiment, we used the RENISHAW linear encoder (Renishaw Co., 2013) which its precise degree is up to 0.1μm and its

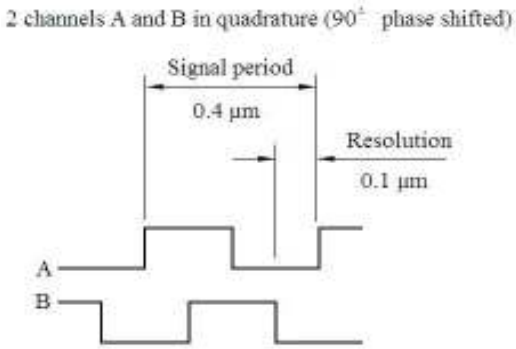

Fig. 12: The stereogram of a long distance piezoelectric actuated stage

characteristics include small size, high resolution, fast response speed and easy installation. Owing to the output signal of the linear encoder is voltage pulse signal, we need to convert it into a position signal to facilitate the follow-up application.

The signal analysis of linear encoder is as shown in Fig. 12 (Sung and Mou, 2008). As we can see, two output signals of linear encoder have 90° phase shifted. Thus we could judge which group of signal phase is in the lead or lag to know the real moving direction of stage. However when output signal is a full cycle square wave, it represents the stage has moved 0.4 μm. There is a 1/4 cycle difference between two signals which represents a minimum resolution of linear encoder is 0.1 μm. The signal of the linear encoder could be acquired by using a digital oscilloscope or a Data Acquisition (DAQ) card and so on. In this study, the DAQ card is used to acquire the position signals and LabVIEW software is used as a human-machine interface to display and read (signals acquire)/write (parameters control) the waveforms. The LabVIEW program of signals acquisition and display is as shown in Fig. 13. Setting the routing channel which is used for acquiring the signal in the DAQ card is as shown in block A of Fig. 13. The parameters adjustment of signal acquisition is including the sampling frequency, the number of samples and the way to acquire the signal, which is as shown in block B of Fig. 13. The display way of acquired signal and its quantity display are as shown in block C of Fig. 13.

The linear encoder signals we acquired from two experiments that represent a moving condition of the stage to left and to right which are shown in Fig. 14(a, b). Besides, we could find out that the signal A leads 90° phase difference than the signal B by comparing two phases of Fig. 14(a). On the other hand, the signal A lags 90° phase difference than the signal B by comparing two phases of Fig. 14(b). As we can discover from Fig. 14(a, b): the reasons why caused the cycle of these two signals unequal include that the moving speed of stage to left and to right is not the same, the piezoelectric actuator is nonlinear effect and

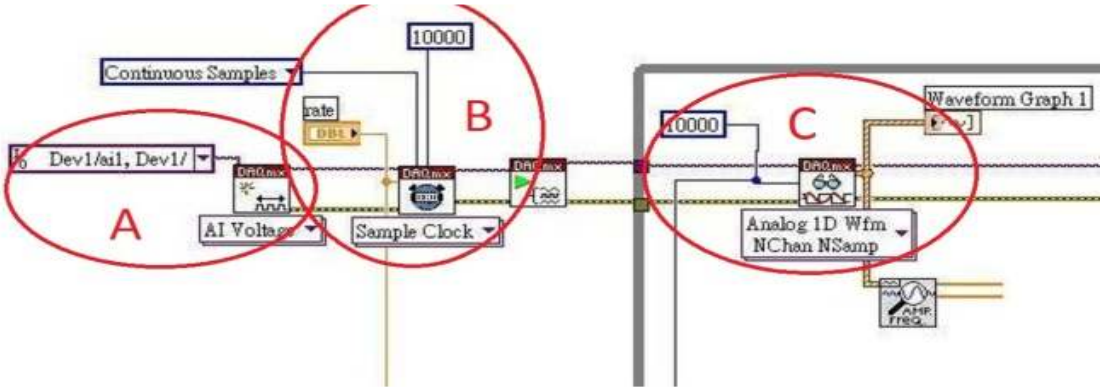

Fig. 13: The LabVIEW program for acquired signals of the linear encoder

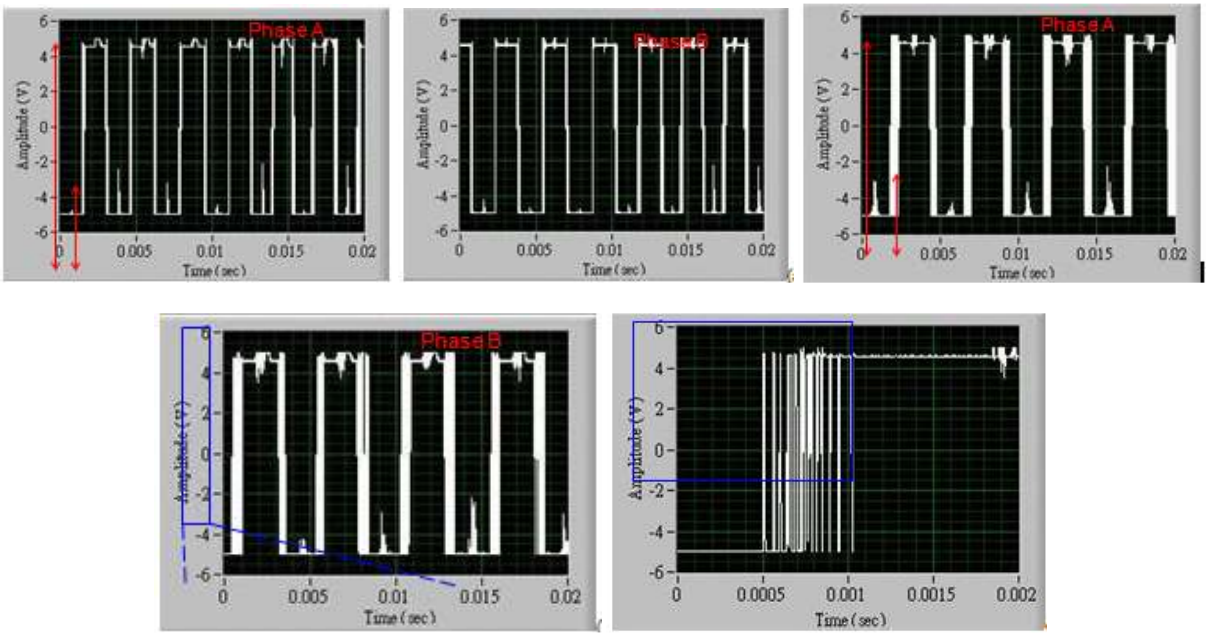

Fig. 14: (a) The signal A of the linear encoder leads 90° phase difference than the signal B by comparing two phases; (b) the signal A of the linear encoder lags 90° phase difference than the signal B; (c) an enlargement figure of the marked area of Fig. 14(b)

the forward rotation and reverse rotation capability of actuator are unbalanced.

The DAQ card we used in this study contain a built-in counter (NI PCI-6115 simultaneous sampling multifunction DAQ) (National Instruments Co., 2013), however there are some problems in judging the correct position signal by using counter. As shown in Fig. 14(b), it's one of the output signals of the linear encoder. According to the normal judgment, the 4 full cycle signals are generated within 0.02 sec which represents the stage has moved 1.6 μm. Because the noise in linear encoder is also calculated by counter, that's why the position signal is larger than 1.6 μm. As shown in Fig. 14(c), it is a figure which is enlarged the marked area of Fig. 14(b). However it should be a signal which is from low potential to high potential, but it has been generated several oscillations and causes some error accumulations of the counter. Moreover, in order to make sure it is a noise interference not a normal signal, we compared Fig. 14(b) with Fig. 14(c) then found out that the oscillation condition would be generated when one side of the signals is from low level to high level; the other side of the signals is just a voltage movement with small margin. As we can see the oscillation condition in Fig. 14(c), it's not a signal of a real position moving. Therefore we must remove the position signal judgment to obtain the correct signal in position moving.

DISTURBANCE FILTER

In a natural environment, plenty of noise interferes with linear encoder signals. For example, an interference signal generated from electronic appliances

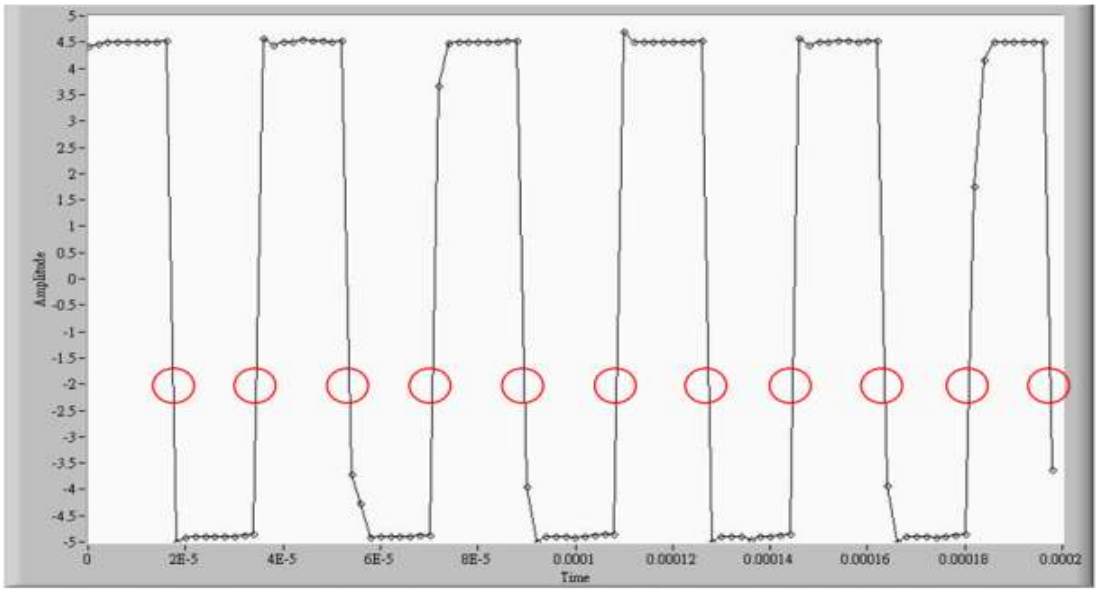

Fig. 15: The LabVIEW program for acquired signals of the linear encoder

or other instruments, interference arising from vibration of a desk surface, extrinsic artificial vibration, or vibration that occurs for any other reasons can_lead to the generation of several vibrations and result in erroneous addition performed by a counter. If the aforesaid problem is not properly handled, a phenomenon will occur, that is, the stage has not moved, but the counter adds up movement position signals continuously, thereby resulting in a lack of precision in the step measurement and positioning control experiments.

With the linear encoder being susceptible to extrinsic interference, it is necessary to process the signals of the linear encoder. Hence, judgment of a position signal should be free from extrinsic interference, in order to obtain the correct position movement signal. Therefore, the LabVIEW program must set forth the means of filtering and the method for retrieving a correct signal.

"Peak Detector VI (virtual instrument)" and "Trigger and Gate VI" are used in the LabVIEW program. "Start Trigger" is adjusted to set the "Gate" value to -2 V. The purpose of not applying +2 V and -2 V simultaneously is to avoid producing repeated data. Hence, the two triggering points +2 V, -2 V are not adopted in the experiment. When a triggering point is set to 0 V, the linear encoder does not end up with moving signals at the moment when the power is turned on as the voltage is zero. At this moment, wrong signals are counted and thus the triggering point 0 V is not adopted. The reason for setting the "Gate" value to -2 V is that, when the stage holds still, the optical scale is subjected to an interference signal that range between +1 V and -1 V. When the stage moves, the signals of the linear "Gate" value is set to +2 V or -2 V. However, based on the encoder always range between +5 V and -5 V. In the experiment, an interference signal is not counted, whether the result of the experiment, the "Gate" value is set to -2 V to obtain the most complete signal of the linear encoder by filtering while the stage is moving. Hence, setting the "Gate" value to -2 V does not contribute to mistake an interference signal for a signal in connection with the moving stage. The "Peak Detector VI" detects the signal of a peak in order to ensure_that a vibration that occurs while the linear encoder is switching between high voltage level and low voltage level will not be repeatedly recorded. The peak values of the processed signals are measured and displayed and each point is counted and calculated, so as to obtain an accurate position signal of the moving stage. This method is similar to the application of a Schmitt trigger circuit. As shown in Fig. 15 (Zhuang and Mou, 2011), when a signal is sent from the linear encoder and passes through the "Gate" value to -2 V, the number of triggers is used as the basis of a count.

CONCLUSION

Most piezoelectric motors employ a multilayer or a stack piezoelectric material. These piezoelectric materials are expensive and thus commercially-available piezoelectric motors are expensive, too. A novel piezoelectric motor developed by our research team is a 4-9-9-14 piezoelectric actuator that comprises an inexpensive piezoelectric buzzer. The purpose of the piezoelectric actuator is to position a stage of a mechanical system in a manner that the movement and positioning of the state can be controlled by varying the driving frequency and driving voltage of the piezoelectric actuator. According to the rotational speed

experiment, the average CW/CCW capability of 4-9-9-14 piezoelectric actuator is probably 1:0.8 and 3-4-5 piezoelectric actuator is probably 1:0.01. The CW/CCW capability of 4-9-9-14 piezoelectric actuator is more balance than 3-4-5 piezoelectric actuator. The 4-9-9-14 piezoelectric actuator comprising a buzzer, as disclosed in this study, applies to a piezoelectric actuated stage designed by our research team.

The movement of the piezoelectric actuated stage is acquired and analyzed by means of LabVIEW software operating in conjunction with a linear encoder. Stage movement-related signals read by the linear encoder are processed. With a human-machine interface of LabVIEW software, the movement of the stage is depicted by a waveform chart to thereby facilitate the observation of the waveform chart and the understanding of propulsion of the piezoelectric actuated stage by the 4-9-9-14 piezoelectric actuator.

The error signal generated from linear encoder could be judged by the LabVIEW program with DAQ card so that it could avoid the malfunction and get a correct position signal. In this study, we used the LabVIEW software to solve the linear encoder problems and replace the control circuit to make the experiment process simpler so that it could save the circuit manufacturing and designing.

REFERENCES

Jheng, S.Y. and S.C. Mou, 2008. Structure design, characteristics measurement and speed control of a CW-CCW-balancing type piezoelectric actuator. MA Thesis, of Ching Yun University, Taiwan.

Juang, P.A. and H.J. Hardtke, 2001. Anewdisc-type ultras onic motor. Sensor. Actuat. A-Phys., 94: 102-111.

Mou, S.C., 2011. System modeling and fuzzy control of a thin-disc type piezoelectric actuator. Adv. Mater. Res., 301-303: 1658-1669.

Mou, S.C., 2012. Structure design, dynamic simulation and characteristic measurement of a thin-disc ultrasonic actuator. Res. J. Appl. Sci. Eng. Technol., 4(20): 3923-3929.

Mou, S.C., 2013. Structure design of the single-axis piezoelectric actuated stage using a 4-9-9-14 piezoelectric actuator. Appl. Mech. Mater., 303-306: 1661-1665.

Mou, S.C. and M.S. Ouyang, 2004. Design, simulation, modeling and analysis of a shaft-driving type ultrasonic motor. Ph.D. Thesis, National Tsing Hua University, Taiwan.

National Instruments Co., 2013. Information on Information on http://sine.ni.com/nips/ cds/view/ p/lang/en/nid/11886.

OBO, 2013. Information on Seahorn Electronic Co., Ltd. Retrieved from: http:// www.obopro2.com/ front/bin/cglist.phtml?Category=3.

Renishaw Co., 2013. Information. Retrieved from: http://www.renishaw.com/ en/renishaw-touch-probes-rotary-encoders-linear-encoders-angle-encoders-laser-calibration-dental-cad-cam-raman-spectroscopy-and-surgical-robots--1030.

Sashida, T. and T. Kenjo, 1993. An Introduction to Ultrasonic Motors. Clarendon Press, Oxford.

Sung, C.H. and S.C. Mou, 2008. Precision positioning control of a long-range piezoelectric actuated stage by fuzzy law. MA thesis, of Ching Yun University, Taiwan.

Ueha, S., Y. Tomikawa, M. Kurosawa and N. Nakamura, 1993. Ultrasonic Motors- Theory and Applications. Clarendon Press, Oxford.

Wen, F.L. and C.Y. Yen, 2007. Design and dynamic evaluation for a linear ultrasonic stage using the thin-disc structure actuator. Ultrasonics, 47: 23-31.

Wen, F.L., C.Y. Yen and M.S. Ouyang, 2003. Thin-disk piezoceramic ultrasonic motor Part I: design and performance evaluation. Ultrasonics, 41: 437-450.

Yen, C.Y., F.L. Wen and M.S. Ouyang, 2003. Thin-disk piezoceramic ultrasonic motor Part II: System construction and control. Ultrasonics, 41: 451-463.

Zhuang, Y.R. and S.C. Mou, 2011. Using fuzzy law and discontinuous clock chain to control a X-Y piezoelectric actuated stage. MA Thesis, of Ching Yun University, Taiwan.